Progress In Electromagnetics Research M, Vol. 104, 133–144, 2021

Characteristic Research on Double Rotor Permanent Magnet Motor with Irregular Halbach Array

Yonglin Pan and Libing Jing*

Abstract—Dual-rotor permanent magnet motor has the characteristics of high torque density and high efficiency and has a wide range of application prospects in many fields. However, the double air-gap structure also makes the internal magnetic field distribution more complicated and torque fluctuation more serious. To improve the double-layer air-gap magnetic field distribution and reduced torque pulsation, based on the Halbach array magnetization, the inner and outer irregular Halbach array dual-rotor permanent magnet motor model was established to obtain the ideal one-sided magnetic field. By comparing the magnetic field distribution of the inner and outer layers, the no-load back-EMF, and the cogging torque, it is proved that the motor with the proposed structure can optimize the air-gap magnetic density and no-load back-EMF and reduce the cogging torque; at the same time, the torque ripple is also significantly reduced to ensure the stability of the motor operation.

1. INTRODUCTION

Dual-rotor permanent magnet motor has two independent stator and rotor structures; inner and outer structures can operate and output independently. It has the advantages of light weight, small size, high efficiency, and long life. Now it is often used in various high-end technologies, such as new energy vehicles, aerospace, wind power generation, and other fields [1, 2]. However, the operation characteristics of the permanent magnet motor determine that it will produce cogging torque and non-ideal air-gap flux density waveform when it is running. The air-gap flux density of the permanent magnet motor largely determines the performance of the back electromotive force and output torque. The dual-rotor permanent magnet motor has two air gaps inside and outside. Therefore, the quality of the air-gap flux density and the fluctuation of the cogging torque have a great impact on the performance of the motor [3–5].

For surface-mounted permanent magnet motors, parallel or radial magnetization is generally used. However for air-gap flux density, whether parallel or radial magnetization, there are always problems such as low sine and high harmonic. In the early stage, Professor Klaus Halbach proposed a special arrangement of magnets — Halbach permanent magnet array. This magnet array can make the magnetic field distribution more sinusoidal, and the magnetic field intensity has a unilateral effect. It also has the characteristics of reducing the cogging torque of the motor and improving stability. Halbach array makes the permanent magnet be used better and greatly improves the utilization rate of the permanent magnet, which has attracted wide attention from the academic community. To make more breakthroughs in this method, domestic and foreign researchers have applied Halbach permanent magnet array to motor design. In [6], the magnetic pole segmentation was proposed. For the single-layer Halbach array, the influence of different block numbers of each pole on the air-gap flux density was compared, and it was concluded that the sinusoidal of Halbach permanent magnet array was affected by the number of magnetic poles blocks. Reference [7] explored the influence of a four-block Halbach array structure of

Received 19 July 2021, Accepted 1 September 2021, Scheduled 3 September 2021
* Corresponding author: Libing Jing (jinglibing163@163.com).
The authors are with the College of Electrical Engineering & New Energy, China Three Gorges University, Yichang 443002, China.

the permanent magnet on the unilateral magnetic concentration of the inner and outer double air gaps. Reference [8] studied three inhomogeneous permanent magnets using Halbach array. In [9], a T-type and claw-type Halbach permanent magnet array was proposed to improve the motor's air-gap flux and power output efficiency.

In recent years, researchers have shifted from single-layer structure to double-layer structure on Halbach permanent magnet array and made a series of studies. In [10], a double-layer Halbach permanent magnet array was used to design a high-speed slotless permanent magnet synchronous motor, and the sinusoidal degree of air-gap flux density was improved by improving the shape and size of the magnet. Reference [11] designed and optimized the magnetization direction of a double-layer Halbach array permanent magnet and compared the sinusoidal degrees of the air-gap flux densities of the single-layer and double-layer Halbach arrays in detail, but there was no discussion and analysis on the size of the permanent magnet. In [12], a permanent magnet motor with a double-layer Halbach array inside and outside was studied. This method made the motor structure more complex and dramatically increased the difficulty of permanent magnet magnetization and machine manufacturing.

In this paper, the shape, arrangement, and combination of permanent magnets of Halbach permanent magnet array are improved based on previous studies. Compared with the traditional double-rotor motor, the parameters of permanent magnet and motor size are the same. A double-rotor permanent magnet motor with irregular topology is designed. The cogging torque, air-gap flux density, back electromotive force, and output torque are simulated by the finite element method. The harmonic analysis of the magnetic field waveform is carried out by Matlab. Compared with the traditional dual-rotor motor, the optimization effect of the irregular topology is verified, namely, the reduction of air-gap harmonics, the improvement of waveform sine, the decline of the cogging torque, the decline of back electromotive force harmonics, and the advancement of waveform sine.

2. MOTOR TOPOLOGY AND OPERATION PRINCIPLE

Figure 1 shows the motor two-dimensional profile. It can be seen that the inner rotor and middle stator constitute the 'inner motor part'; the outer rotor and middle stator constitute the 'outer motor part'; and the double rotor motor is composed of the inner and outer motors.

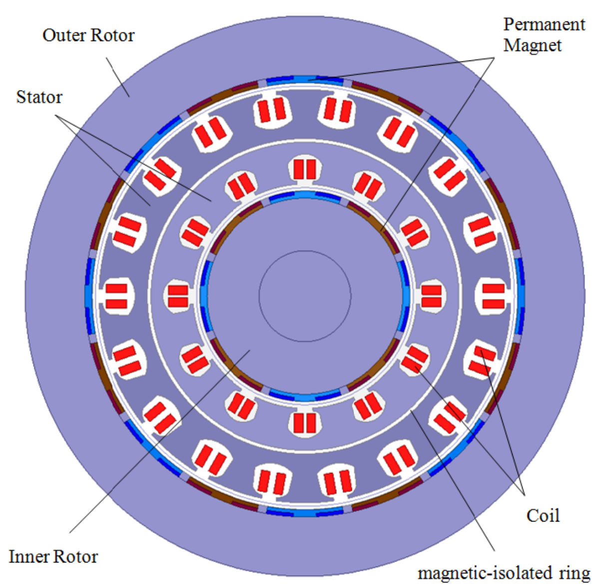

Figure 1. Motor structure.

The two sides of the stator are slotted respectively, and the armature winding is connected to two motor units through the stator. Due to the magnetic isolation ring, the inner rotor and outer rotor constitute the inner motor unit and outer motor unit respectively with the middle stator. Under the action of three-phase alternating current, the magnetic field of stator winding interacts with the magnetic field generated by the permanent magnet of the inner and outer rotors, and the electromagnetic torque drives the output mechanical energy of the inner and outer rotors [13, 14].

2.1. Traditional Halbach Array

In Halbach magnet magnetization, the magnetic field similar to sinusoidal distribution is the most ideal [15–17], but it is difficult to achieve in engineering manufacturing. In order to obtain the sinusoidal magnetic field, the permanent magnet is usually segmented, and then each segment of the permanent magnet is changed to the appropriate magnetization direction. The magnetization direction of permanent magnet is shown in Fig. 2. The permanent magnet installation of the motor is generally circular. Fig. 3 shows the magnetization direction of the Halbach array with three blocks per pole. The direction of magnetization and the number of magnet blocks are as follows [18]:

$$\theta = (1 \pm p) \times \theta_i \tag{1}$$

where θ is the magnetization angle of the i-block permanent magnet. θ_i is the angle between the geometric centerline of the i-block permanent magnet and the transverse coordinate. '+' represents the 'outer rotor', and '−' represents the 'inner rotor'. p represents the pole number of the motor.

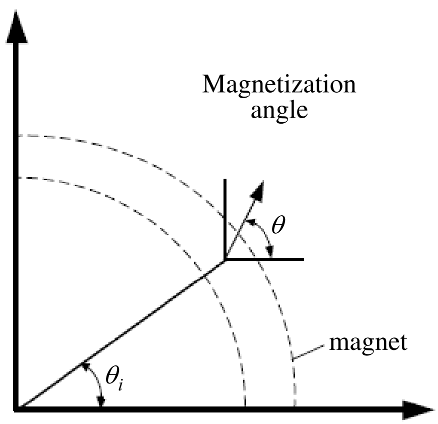

Figure 2. Magnetization direction of Halbach array magnets.

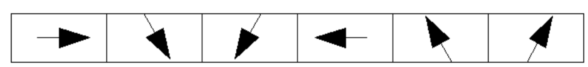

Figure 3. Magnetization direction of three Halbach arrays per pole.

2.2. Advanced Halbach Array

In this paper, a new Halbach array structure is used, and the whole permanent magnet is divided into three pieces as shown in Fig. 4.

This part of the Halbach array has the same number of permanent magnets as the ordinary Halbach array. However, the number of permanent magnets used by the former is significantly reduced compared with that of the latter, and the structure has also been changed. The main magnetic pole is a convex permanent magnet, and the vice magnet poles on both sides are two permanent magnets for magnetic gathering [19]. Each part of the permanent magnet is magnetized in a specific direction to achieve magnetic gathering to the stator slot side.

3. FINITE ELEMENT ANALYSIS

In this paper, a dual-rotor permanent magnet motor with an inner rotor of 12 slots and 8 poles and an outer rotor of 18 slots and 16 poles is selected as an example, and Table 1 shows the main parameters of the motor.

In order to compare the performances of each parameter between the Halbach magnetization of the new structure and the traditional radial magnetization. The permanent magnet materials are

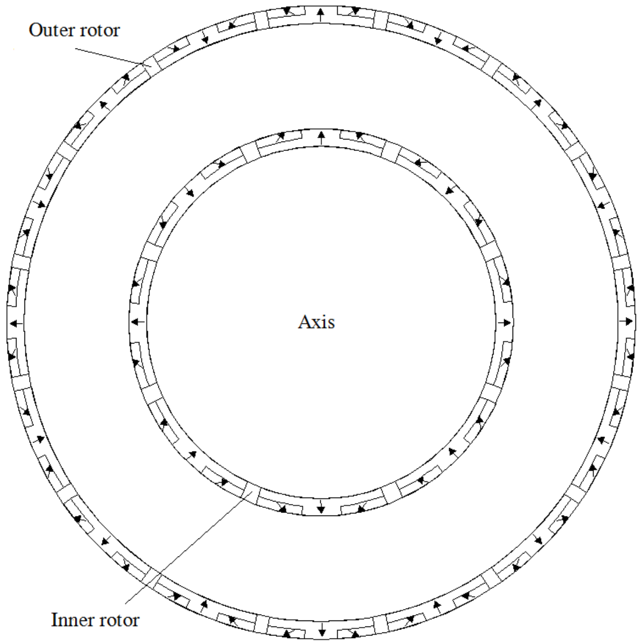

Figure 4. Magnetic direction of Halbach array.

Table 1. Parameters of double rotor motor.

Parameter	Value	
	Inner rotor	Outer rotor
Umber of pole-pairs	4	8
Slot number	12	18
Groove angle (°)	8	4
Stator inner radius (mm)	32	44
Stator outer radius (mm)	45	59
Rotor inner radius (mm)	13	63
Rotor outer radius (mm)	28	80
Permanent magnet inner radius (mm)	28	61
Permanent magnet outer radius (mm)	30	63
Motor length (mm)	65	65
Pole-arc factor	0.889	0.889

NdFeB; the shape, size, and style are consistent; and the thickness is 2 mm. However, the amount of new structure Halbach magnet is less than the traditional magnet, which reduces the cost of motor manufacturing. Each pole is divided into three small blocks, and Halbach magnetic field is used. At the stator slot, the rectangular slot of the traditional motor is changed to the arc slot, as shown in Fig. 5.

The low saturation of the magnetic circuit can not only improve the power density of the motor, but also greatly reduce the iron loss of the motor during operation. As shown in Fig. 6, the magnetic flux densities of each part of the motor before and after improvement are roughly the same, and the inner magnetic field meets the allowable range of the core material used. It is obvious that the magnetic flux density of the arc slot is lower than that of the rectangular slot, which is beneficial to improve the operational stability and control accuracy of the motor.

The magnetic flux density of the motor is shown in Fig. 7. Fig. 7(a) shows the traditional motor

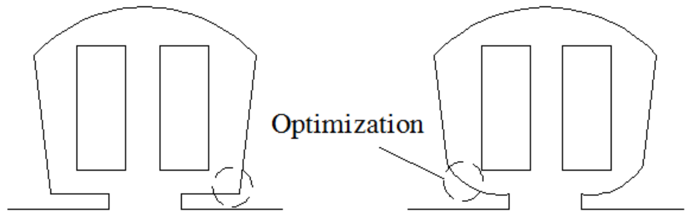

Figure 5. Comparison of slot improvement.

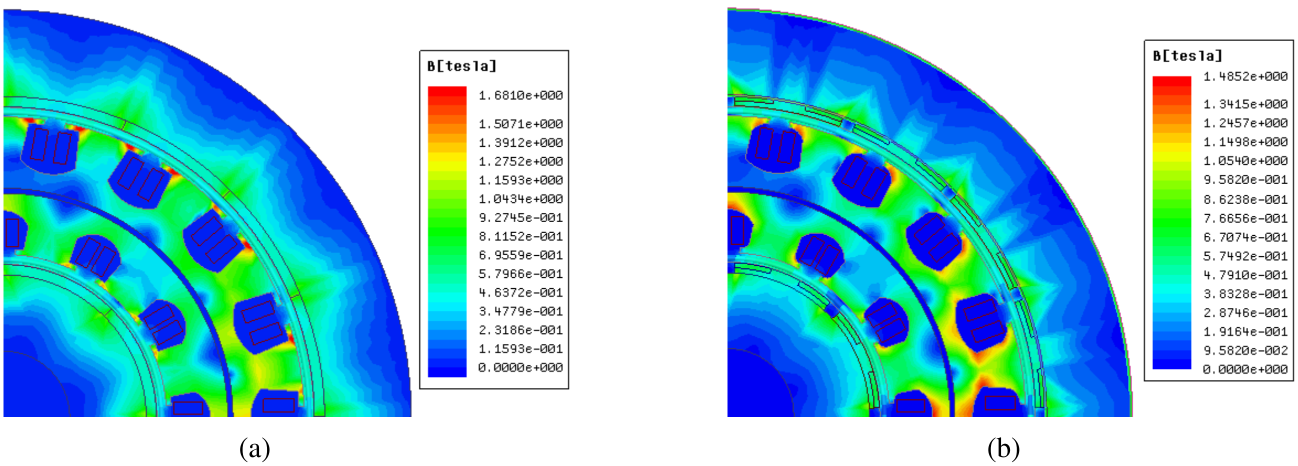

Figure 6. Magnetic flux density nephogram of motor. (a) Traditional; (b) Proposed.

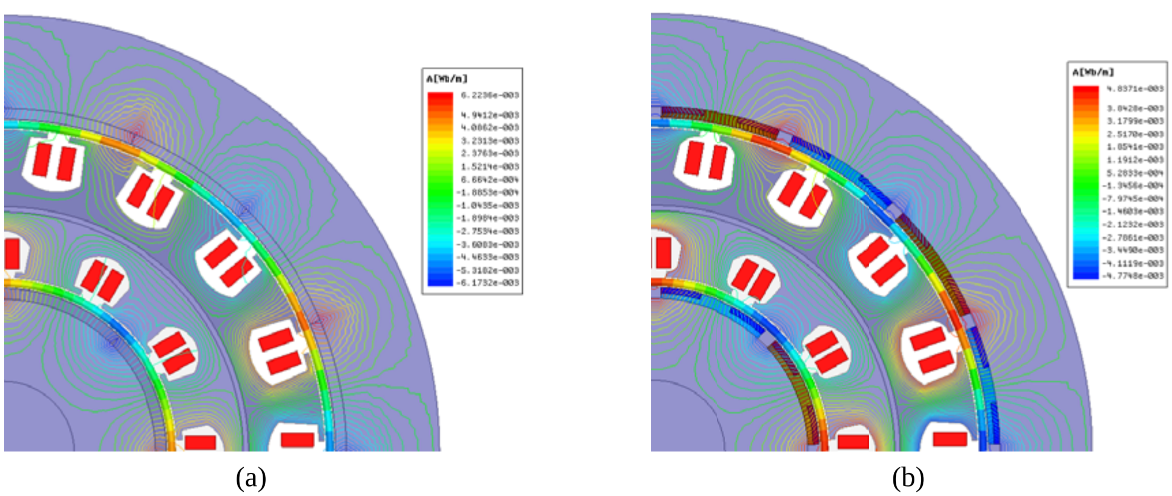

Figure 7. Motor profile. (a) Traditional; (b) Proposed.

model, and Fig. 7(b) shows the new partial Halbach magnetization model. It can be seen that due to the existence of the magnetic isolation ring, the internal and external magnetic circuits of the motor are independent of each other, and they are coupled with each other in the circuit. The magnetic line of the new structure is smoother and not dense, which reduces the heat production of the motor [20].

3.1. Analysis of Radial Magnetic Density

For a permanent magnet motor, the air-gap flux density waveform directly affects the magnetic flux per pole of the motor, and then affects the noise and working characteristics of the motor. Therefore, the higher the sine degree of the air-gap flux density waveform of the inner and outer motor is, the better the effect is. The radial air-gap flux density waveforms of traditional and proposed structures are compared below.

As shown in Fig. 8(a), the sinusoidal waveform of air-gap flux density generated by the new partial Halbach array is relatively better. As shown in Fig. 8(b), due to the relative reduction of the amount of the proposed permanent magnet, the fundamental amplitude is slightly reduced to normal, and the 12th and 20th harmonics are significantly reduced.

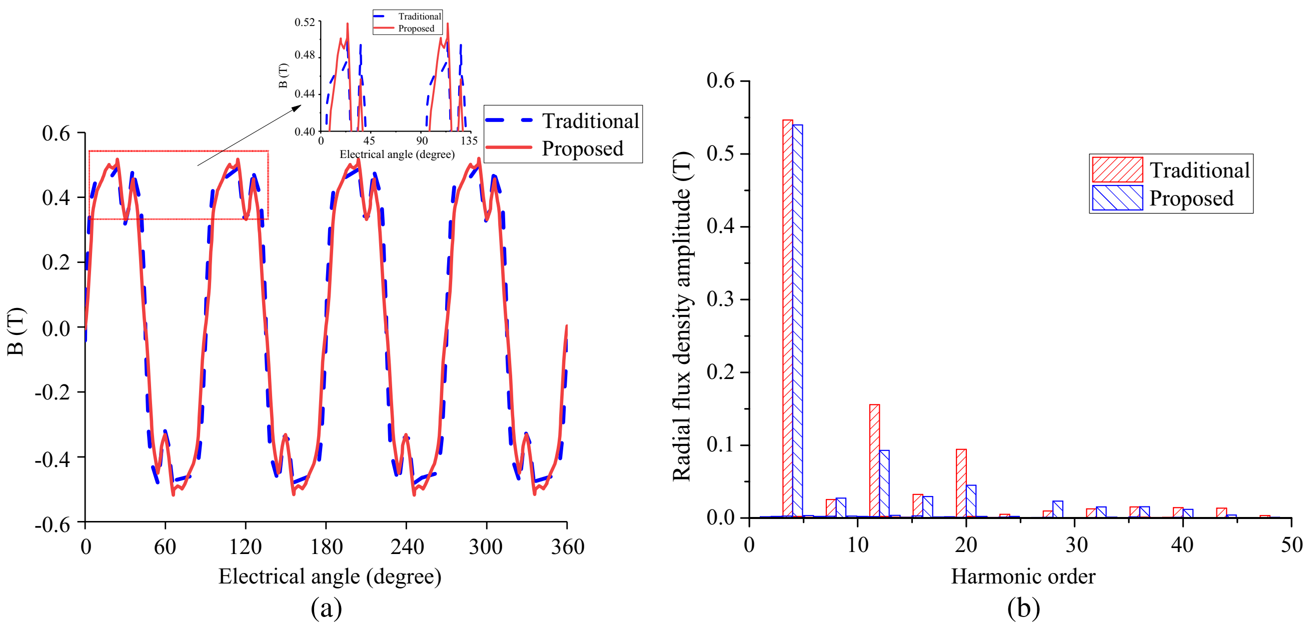

Figure 8. Comparison of inner layer radial flux density. (a) Flux density waveform; (b) Harmonic spectra.

As shown in Fig. 9(a), the proposed Halbach array structure has a unilateral magnetic concentration effect, which produces a higher amplitude of the air-gap flux density basis wave and a better sine. As shown in Fig. 9(b), the fundamental amplitude is slightly reduced to normal due to the relative reduction in the amount of the proposed permanent magnet, and the 12th and 20th harmonics are significantly reduced.

Harmonic is difficult to eliminate in the actual operation of the motor, so the sine of the air-gap flux density waveform before and after the improvement is reflected by the size of the harmonic distortion rate and expressed by THD, that is:

$$\mathrm{THD} = \frac{\sqrt{\sum_{k=2}^{\infty} B_k^2}}{B_1} \times 100\% \tag{2}$$

where B_k is the kth harmonic amplitude, and B_1 is the fundamental amplitude.

It can be seen from the above equation that the harmonic distortion rate directly affects the high-order harmonic content of air-gap flux density. The higher the harmonic distortion rate is, the higher the high-order harmonic content is, and the lower the fundamental wave content is. The harmonic distortion rate before and after the improvement can be obtained as the data in Table 2. The improved part of the Halbach array magnetized motor has low THD value and less harmonic content.

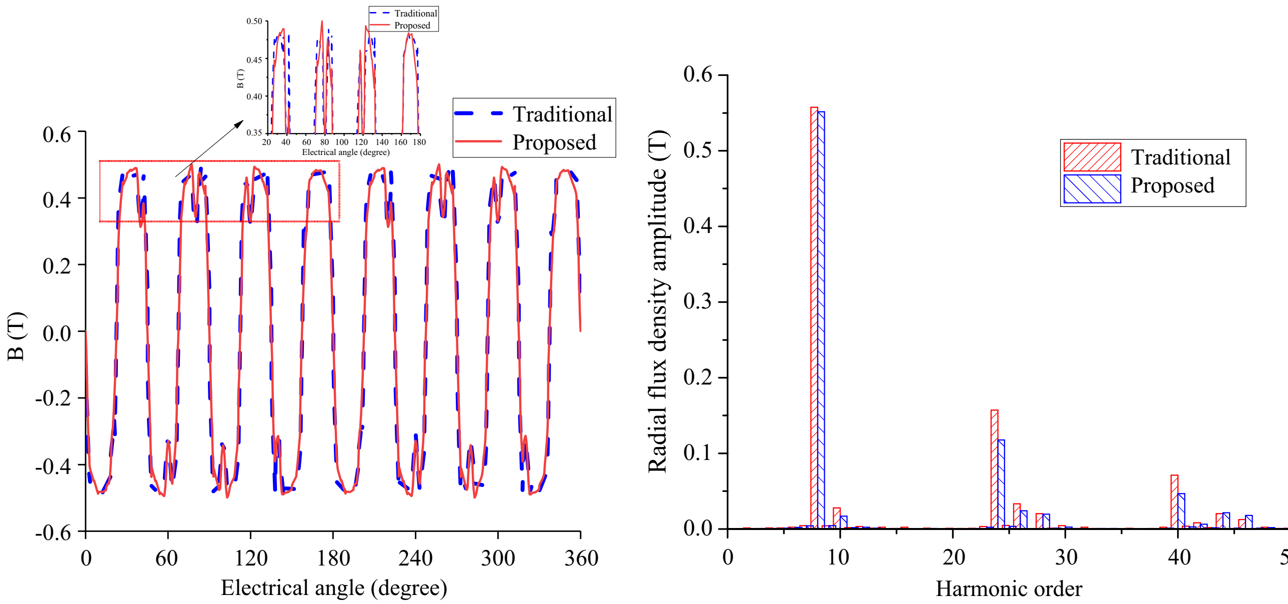

(a) (b)

Figure 9. Comparison of outer layer radial flux density. (a) Flux density waveform; (b) Harmonic spectra.

Table 2. Comparison of harmonic distortion rate of air-gap flux density.

Structure	THD (%)	
	Inner rotor	Outer rotor
Traditional	34.63	32.51
Advanced	21.60	24.46

3.2. Analysis of Cogging Torque

Due to the structure of the permanent magnet motor itself, there is always cogging torque. The cogging torque will make the motor produce not only noise, but also vibration, which will directly affect the overall control accuracy of the motor. Therefore, it is particularly important to study the generation and optimization of the cogging torque in the design of a permanent magnet motor. The attraction between the permanent magnet and the cogging generates cogging torque. The cogging torque in the permanent magnet motor changes periodically with the change of the relative position of the magnet pole and the tooth.

The motor cogging torque formula is as follows:

$$T_{cog} = -p\frac{W(\alpha)}{\partial \alpha} \tag{3}$$

where α is the rotor angle (electric angle). W is the total energy of air-gap magnetic field. p is the polar logarithm. W may indicate:

$$W(a) = W_{ag}(a) = \frac{1}{2m_0}\int_v B^2 dV \tag{4}$$

The parameters of the dual-rotor permanent magnet motor given above are used as the model for analysis. The specific method is to ensure that the inner and outer rotors of the motor rotate in opposite directions. In order to simulate the open circuit of the winding, the winding current amplitude in the middle stator slot is set to zero, and then other conditions are kept unchanged. The magnetization direction of the permanent magnet is changed from radial magnetization to partial Halbach array

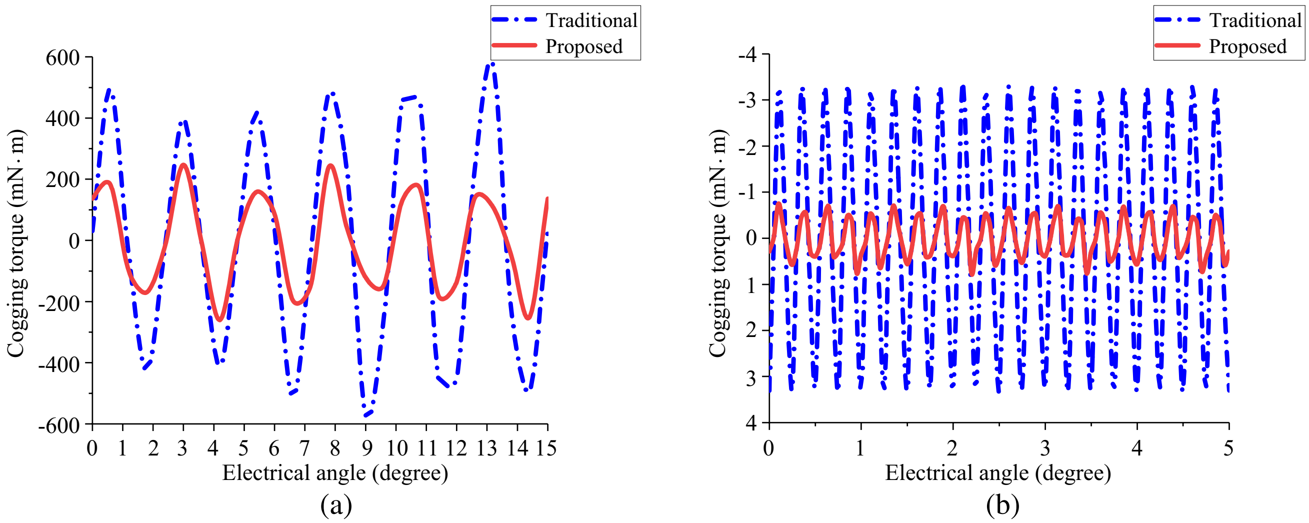

Figure 10. Comparison of the cogging torque waveform. (a) Inner rotor; (b) Outer rotor.

magnetization, and then the cogging torque under two magnetization modes is calculated by finite element model in Maxwell simulation software for comparison. Fig. 10(a) and Fig. 10(b) show the comparison of the cogging torque waveform between the traditional motor and the new partial Halbach.

It can be seen from Fig. 10 that in the inner rotor motor, the cogging torques of the traditional radial magnetization and partial Halbach array magnetization are 572 mN·m and 246 mN·m, respectively, and the cogging torque is reduced by about 57%. In the outer rotor motor, the cogging torques of traditional radial magnetization and partial Halbach array magnetization are 3.3 N·m and 777 mN·m, respectively, and the cogging torque is reduced by about 77%. Therefore, the new partial Halbach array can effectively reduce the cogging torque of the permanent magnet motor.

3.3. Analysis of Back-EMF

Figures 11 and 12 are the back-EMF waveform and harmonic comparison diagrams before and after improvement. From the figures, it can be seen that the motor with the new partial Halbach array has a more sinusoidal back-EMF waveform. In the back-EMF fundamental amplitude, the fundamental amplitude of the proposed structure is slightly reduced. However, due to the reduction of the use of the permanent magnet, it is normal here, and the high-order harmonics are significantly lower than before, so the overall performance is better than before.

3.4. Analysis of Torque

In this paper, the torque fluctuation coefficient k_T is calculated by the stall method, which is defined as follows:

$$k_T = \frac{T_{\max} - T_{\min}}{T_{\max} + T_{\min}} \times 100\% \tag{5}$$

where $T_{\max}$ and $T_{\min}$ are the maximum torque and minimum torque in the output torque.

The inner and outer rotors rotate in opposite directions, and the output torque of the permanent magnet radial magnetization and partial Halbach magnetization is shown in Fig. 13.

The torque ripple coefficient is 40.85%, and the average output torque is −1.241 N·m under the radial magnetization of the inner rotor. In the case of partial Halbach array magnetization, the inner rotor torque ripple coefficient is 19.05%, and the average output torque is −1.209 N·m. The torque ripple coefficient is 73.26%, and the average output torque is 4.528 N·m. In the case of partial Halbach array magnetization, the outer rotor torque ripple coefficient is 16.89%, and the average output torque is 4.485 N·m. The calculation results show that the torque ripple of the improved motor, whether the inner rotor or the outer rotor, is significantly improved, and the stability of the motor is greatly improved.

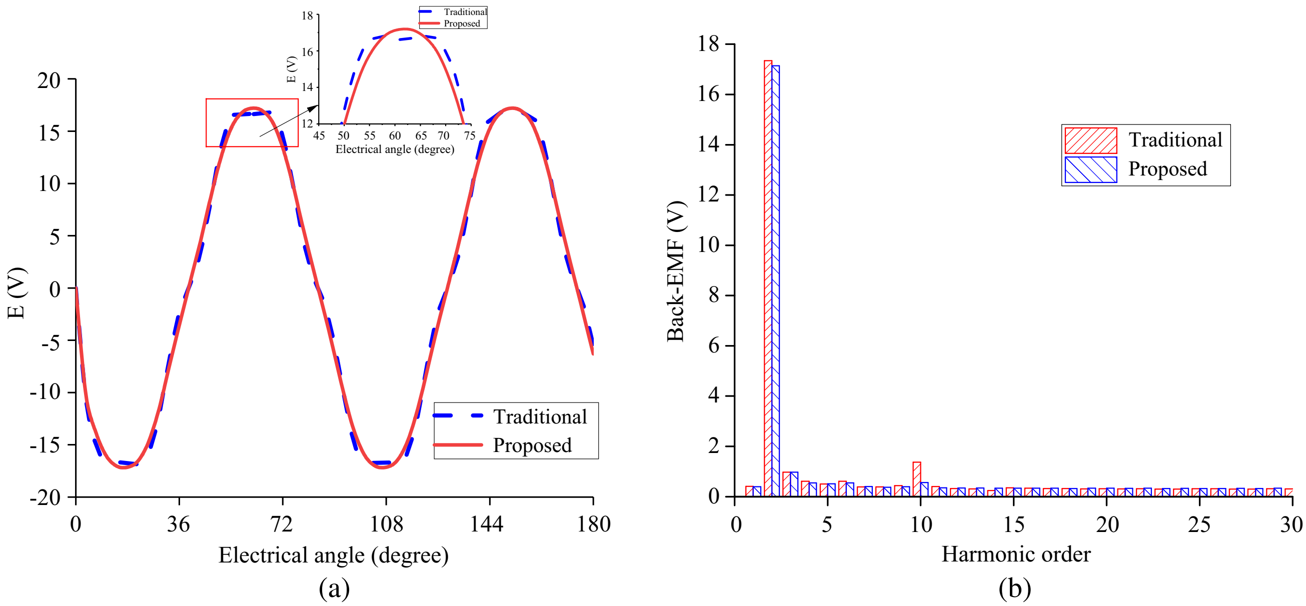

Figure 11. Comparison of inner back electromotive force. (a) Phase back-EMF; (b) Harmonic spectra.

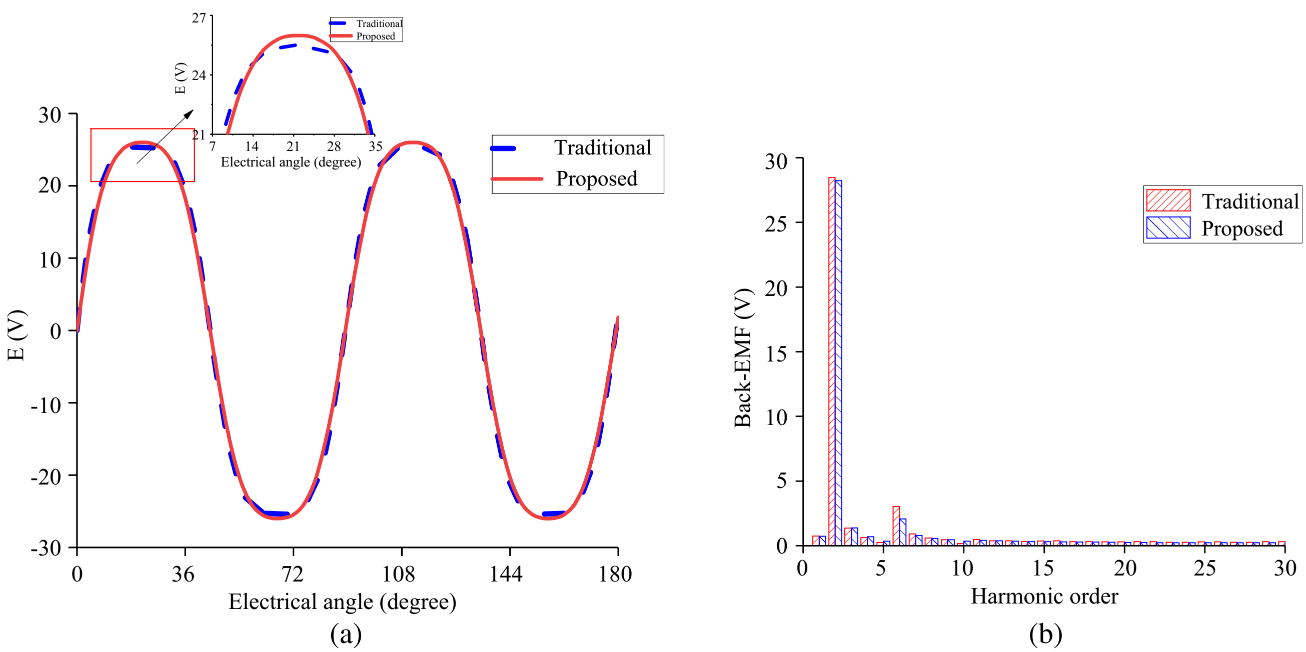

Figure 12. Comparison of outer back electromotive force. (a) Phase back-EMF; (b) Harmonic spectra.

3.5. Analysis of Loss

The electromagnetic loss of the motor is divided into copper loss and core loss. Since the stator winding is the same before and after improvement, the copper loss before and after improvement is 36.3 W. Fig. 14 shows the no-load core loss curve of the motor. It can be seen from the figure that the core loss of the improved motor is less than that before the improvement, so the operation efficiency of the motor is improved.

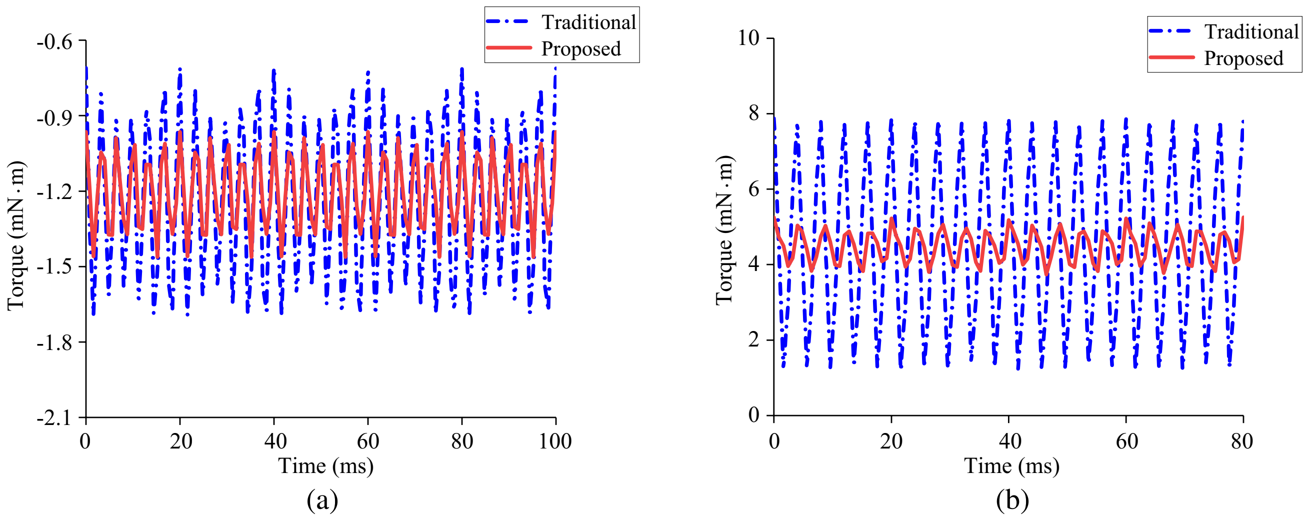

Figure 13. Comparison of torque waveform. (a) Inner rotor; (b) Outer rotor.

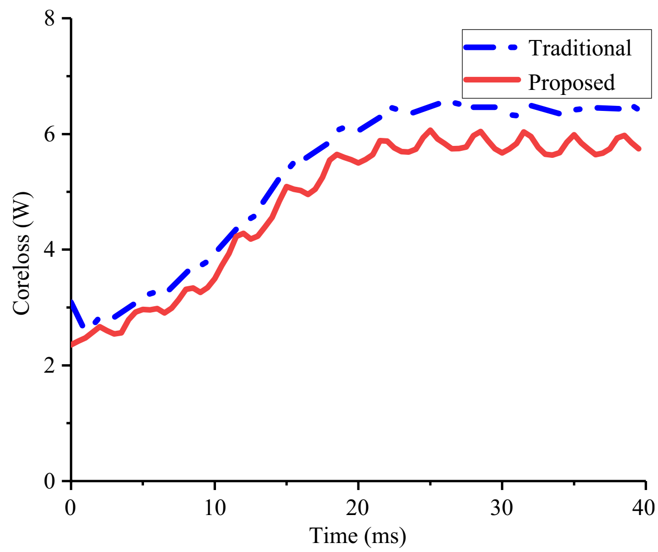

Figure 14. Core loss of motor.

4. CONCLUSION

In this paper, a two-dimensional finite element model of dual-rotor permanent magnet motor is established, and the effects of radial magnetization and irregular Halbach array magnetization on the structure of dual-rotor permanent magnet motor are compared in detail. The air-gap flux density, cogging torque, back-EMF, and output torque ripple of the motor model are used as the basis for the optimization design, and the finite element simulation of the motors with two structures is carried out. The results are as follows:

(1) The Halbach array with suitable angle is used to magnetize the inner and outer permanent magnets of the double-rotor motor by single-side focusing method, so that the inner and outer air-gap flux density of the motor has a more perfect sine, and the improved structure has been greatly optimized on the harmonic component of the radial flux density.

(2) The cogging torque of the inner rotor was optimized from 572.3 mN·m to 246.9 mN·m, which was reduced by 56.9%. The cogging torque of the outer rotor was optimized from 3.31 N·m to 777.02 mN·m,

which was reduced by 76.5%. And the improved inner and outer back-EMF waveform has better sine than radial magnetization, and better weakens the high harmonic content.

(3) The torque ripple coefficient of the inner rotor was optimized from 40.85% to 19.05%. The torque ripple coefficient of the outer rotor was optimized from 73.26% to 16.89%. The reduction of the torque ripple will greatly improve the operation characteristics of the motor, and the reduction of loss also improves the efficiency of the motor. After improvement, the reduction of the amount of inner and outer permanent magnets is also a significant advantage, which effectively reduces the manufacturing cost while ensuring its operational requirements.

REFERENCES

1. Chen, Y. Y., L. Quan, X. Y. Zhu, H. Wei, and W. Zheng, "Electromagnetic performance analysis of double-rotor stator permanent magnet motor for hybrid electric vehicle," *IEEE Transactions on Magnetics*, Vol. 48, No. 11, 4204–4207, 2012.
2. Gao, Q. X., "Optimal design and electromagnetic analysis of double rotor permanent magnet machine," *China Three Gorges University*, 2018.
3. Zhao, W. L., T. A. Lipo, and B. I. Kwon, "Comparative study on novel dual stator radial flux and axial flux permanent magnet motors withferrite magnets for traction application," *IEEE Transactions on Magnetics*, Vol. 50, No. 11, 1–4, 2014.
4. Sun, Y. P., B. K. Su, and X. D. Sun, "Optimal design and performance analysis for interior composite-rotor bearinglesspermanent magnet synchronous motors," *IEEE Access*, Vol. 7, 7456–7465, 2019.
5. Zhang, W. J., S. D. Huang, J. Gao, R. Li, and L. T. Dai, "Electromagnetic torque analysis for all-harmonic-torque permanent magnet synchronous motor," *IEEE Transactions on Magnetics*, Vol. 54, No. 11, 1–5, 2018.
6. Bao, X. P. and Z. Ji, "Structure study and optimization design on Halbach PMSM," *Small & Special Electrical Machines*, Vol. 42, No. 5, 20–25, 2014.
7. Gao, Q. X., C. Wang, L. B. Jing, and Z. H. Luo, "Magnetic field analysis and torque calculation of double-rotor permanent magnet motor with Halbach array," *Small & Special Electrical Machines*, Vol. 46, No. 11, 51–54, 2018.
8. Yang S. and Z. Q. Zhu, "Investigation of permanent magnet brushless machines having unequal-magnet height pole," *IEEE Transactions on Magnetics*, Vol. 48, No. 12, 4815–4830, 2012.
9. Zhang, J., X. M. Liu, and Z. C. Shi, "Design and analysis of alinear generator with improved Halbach PM arrays," *Small & Special Electrical Machines*, Vol. 46, No. 2, 23–26, 2018.
10. Kou, B. Q., H. C. Cao, W. L. Li, and X. C. Zhang, "Analytical analysis of anovel double layer Halbach permanent magnet array," *Transactions of China Electrotechnical Society*, Vol. 30, No. 10, 68–76, 2015.
11. Zhao, C. H., H. F. Cai, and J. Guo, "Comparative research of T raditionalHalbacharray and double Halbacharray," *Journal of Shanghai Dianji University*, Vol. 18, No. 3, 158–162, 2015.
12. Praveen R. P., M. H. Ravichandran, V. T. Sadasivan Achari, V. P. Jagathy Raj, G. Madhu, and G. R. Bindu, "A novel slotless Halbach-array permanent-magnet brushless DC motor for spacecraft applications," *IEEE Transactions on Industrial Electronics*, Vol. 59, No. 9, 3553–3560, 2012.
13. Xu, H., "Reserach on dual-rotor permanent magnet motor," *Changchun University of Science and Technology*, 2014.
14. Huang, Y. K., T. Zhou, J. N. Dong, B. C. Guo, and L. Zhang, "An overview on developments and researches of axial flux permanent magnet machines," *Proceedings of the CSEE*, Vol. 35, No. 1, 192205, 2015.
15. Som, D., K. Li, J. Kadel, J. Wright, S. Modaresahmadi, J. Z. Bird, and W. William, "Analysis and testing of acoaxial magnetic gearbox with flux concentration Halbach rotors," *IEEE Transactions on Magnetics*, Vol. 53, No. 11, 1–6, 2017.

16. Zhang, T., X. T. Ye, L. H. Mo, and Q. Lu, "Electromagnetic performance analysis on the bearingless permanent magnet synchronous motor with Halbach magnetized rotor," *IEEE Access*, Vol. 7, 121265–121274, 2019.
17. Guo, F., Y. J. Tang, L. Ren, and J. Li, "Structural parameter optimization design for Halbach permanent maglev rail," *Physica C: Superconductivity*, Vol. 470, No. 20, 1787–1790, 2010.
18. Liu, L. and L. B. Jing, "Analysis and calculation of the cogging torque of Halbach array permanent magnet machine," *Journal of Magnetic Materials and Devices*, Vol. 47, No. 2, 48–52, 2016.
19. Ni, Y. Y., X. Jiang, B. X. Xiao, and Q. J. Wang, "Analytical modeling and optimization of dual-layer segmented Halbach permanent-magnet machines," *IEEE Transactions on Magnetics*, Vol. 56, No. 5, 1–11, 2020.
20. Choi, J. Y., S. H. Lee, K. J. Ko, and S. M. Jang, "Improved analytical model for electromagnetic analysis of axial flux machines with double-sided permanent magnet rotor and coreless stator windings," *IEEE Transactions on Magnetics*, Vol. 47, No. 10, 2760–2763, 2011.